Revisiting the impact of climate change on agriculture through spatially-varying and place-tailored Ricardian estimates

Noé J Nava[1, 2, *], Sandy Dall'Erba[1, 2], Chang Cai[1, 2], and A. Stewart Fotheringham[3]

[1]Department of Agricultural and Consumer Economics, University of Illinois at Urbana-Champaign
[2]Regional Economics Applications Laboratory (REAL), University of Illinois at Urbana-Champaign
[3]School of Geographical Sciences and Urban Planning, Arizona State University
[*]Corresponding author: Noé J Nava, noejn2@illinois.edu

April 2, 2021

Abstract

The Ricardian framework has been widely used to study the impact of climate change on agriculture across US counties over the past few decades. While the spatial heterogeneity of climate change is well-accepted, the literature struggles to reach an agreement on how to model it, hence leading to a wide range of forecasted impacts. This paper employs Multiscale Geographically-Weighted-Regression (MGWR) to avoid setting an a priori definition of heterogeneity and to generate county-specific marginal effects of climate change impacts. We start with a cross-validation exercise that demonstrates the superiority of MGWR over previous specifications. The local parameter estimates derived from MGWR are then used to forecast changes in farmland value due to expected 2038-2070 climate conditions. Results reveal an expected national average loss in farmland value that is substantially larger than the losses predicted in previous studies. We attribute the divergence to unspecified heterogeneity that leads to a downward bias in farmland price forecasts. While previous studies find a large number of counties benefiting from climate change, our results indicate that only a total of 24 counties – mostly in Texas - will experience gains. Our place-specific marginal effects will help guide the development of place-tailored mitigation and adaptation strategies to climate change.

Keywords: Ricardian approach, agricultural production, farmland value, multiscale geographically weighted regression, hedonic model.

1 Introduction

The estimation of damages from global warming, particularly in the agricultural sector, is receiving an increasing amount of attention. The Ricardian approach, a reduced-form hedonic analysis developed by Mendelsohn et al. (1994) to calibrate such an impact over a single cross-section of data, has been extensively employed to predict climate-change-induced damages on agriculture across spatial units (farms, municipalities, regions) of the country under study, including the U.S. (Schlenker et al., 2005; Schlenker and Roberts, 2006; Dall'erba and Domínguez, 2016), China (Liu et al., 2004; Wang et al., 2009) and South-Africa (Gbetibouo and Hassan, 2005).[1] Despite this substantial coverage, the functional form of the model employed when measuring the consequences of climate change on U.S. agriculture diverges widely across studies. A concern here is the global nature of the marginal effects commonly used in such models.

Current models used to predict the impact of climate change on agricultural production are almost exclusively global, meaning that the responses to a change in climatic conditions are assumed to be the same across whatever country is being analyzed. Early contributions of the Ricardian literature (see the work of Mendelsohn et al. (1994) and Mendelsohn and Dinar (2003)) have been criticized for not fully accounting for region-specific features and for implying that similar changes in agricultural production take place after a 1°C rise in temperature in places as diverse as Florida and Minnesota. Subsequent studies, such as Schlenker et al. (2005), Schlenker and Roberts (2006), Deschênes and Greenstone (2012), and Dall'erba and Domínguez (2016), have remedied this shortcoming by offering various grouping strategies for counties, such as irrigated vs. rainfed counties, high- vs. low-elevated counties, and applying a model separately for each grouping. These approaches allow the generation of between two and fifty different marginal effects for each covariate. However, a misspecified clustering of spatial units could yield mixed and misleading results. In addition, a recent study by Cai and Dall'Erba (2021) indicates that among the county groupings chosen in the literature, there is little evidence for the superiority of one grouping over others.

[1] For an exhaustive review of these Ricardian applications see Mendelsohn and Massetti (2017).

A potential solution to this confusion is to generate spatially varying estimates without any a priori clustering of counties via local regression techniques so that clear county-specific marginal effects can be calculated and place-tailored mitigation strategies can derived from them. Several empirical applications of local regression techniques have outperformed global approaches in terms of their predictive power (see, among others Páez et al. (2008), Zhang et al. (2011) and Soler and Gemar (2018)). However, few applications of local regression models focus on agriculture and, when they do, their outcome variable is crop yield.[2] Consequently, spatial heterogeneity in the marginal effects of climate change has been underexplored. As such, this paper seeks to contribute to both the local regression and the Ricardian literature by addressing this shortcoming. We focus on the United States, a country that has been subject to a large number of previous county-level studies with which we can compare our approach using the newly-developed Multiscale Geographically Weighted Regression (MGWR) framework (Fotheringham et al., 2017).

In the next section, we develop the conceptual framework of our spatial non-stationary Ricardian-approach that extends the original idea of Mendelsohn et al. (1994) to a local, multiscale-structure. We describe in section 3 the data employed in our estimations and forecasts. Contrary to the a priori clustering approaches adopted by previous studies, MGWR allows us to be agnostic about any possible clustering of counties in terms of their response to climate change. In order to show the appeal of this approach to our case study, we employ in section 4 a cross-validation approach on the 2017 data. Results provide evidence of the relative superiority of our local approach compared to any previous specification. In section 5 we describe our forecast results and how they compare to estimates from previous specifications. Our MGWR predictions of the impact of climate change on agricultural production generate an average expected loss of -$2,239.86 [-$4,609.6, $243.29] per acre of farmland value by mid-century across the nation, which is substantially larger than the forecasts from any previous global specification. In addition, previous studies find a large number of counties that will benefit from climate change. Our results contrast with previous findings demonstrating that only a handful

[2]See for example Cai et al. (2014), and Shiu and Chuang (2019).

of counties, mostly located in Texas, will benefit from climate change. Finally, section 6 summarizes the main results and provides some concluding remarks.

2 Spatial non-stationary Ricardian-approach

The idea at the core of the Ricardian approach is that landowners adapt their production choices to new climate conditions. The decisions made vis-à-vis the optimal use of the land are reflected in the land price which is commonly modeled as the discounted sum of future net returns (Mendelsohn et al., 1994; Plantinga et al., 2002):

$$V_i = \int \pi_i^*(t) e^{-rt} dt \tag{1}$$

where V_i is farmland value, π_i^* is the optimal net returns to land at location i, and r is the discount rate. Net returns are a function of the product of the land's output market price P_k and a vector of input prices w, and they depend also on a set of exogenous variables and different land uses denoted as k (Hsiang, 2016); $\mathbf{z}_i = (\mathbf{C}_i, \mathbf{G}_i, \mathbf{S}_i)$ that consists of climate attributes $\mathbf{C}_i$, socio-economic characteristics $\mathbf{G}_i$, and soil quality indicators $\mathbf{S}_i$:

$$\pi_i^* = max_{k\epsilon\{1,\dots,K\}} \pi_{ik}(P_k, \mathbf{w}, \mathbf{z_i}) \tag{2}$$

In this framework, the effect of climate change on farmland values can be conceptualized in panel (a) of Figure 1. Note that the x-axis focuses on changes in temperature, but a similar approach could be used for changes in precipitation. The three overlapping parabolas represent the envelope formed by three different types of land use reflecting that as temperature increases, farmers would choose to switch their inputs and outputs to maximize the land's net return (y-axis left) for a given temperature level. The land value this process leads to (y-axis right) is reflected in the outer parabola for the entire range of temperature. Traditionally, Equation (1) is parametrized through the econometric model depicted in Equation (3) where ($\boldsymbol{\beta_1'}$, $\boldsymbol{\beta_2'}$, $\boldsymbol{G}$, $\boldsymbol{\theta}$) is a set of exogenous coefficients.[3]

[3]Based on their approach, Mendelsohn et al. (1994) forecast that global warming may bring average gains to U.S. agriculture. Since then, their pioneering work has led to a surge of studies using a variation of the Ricardian approach, either in the U.S. or abroad (Mendelsohn and Massetti, 2017).

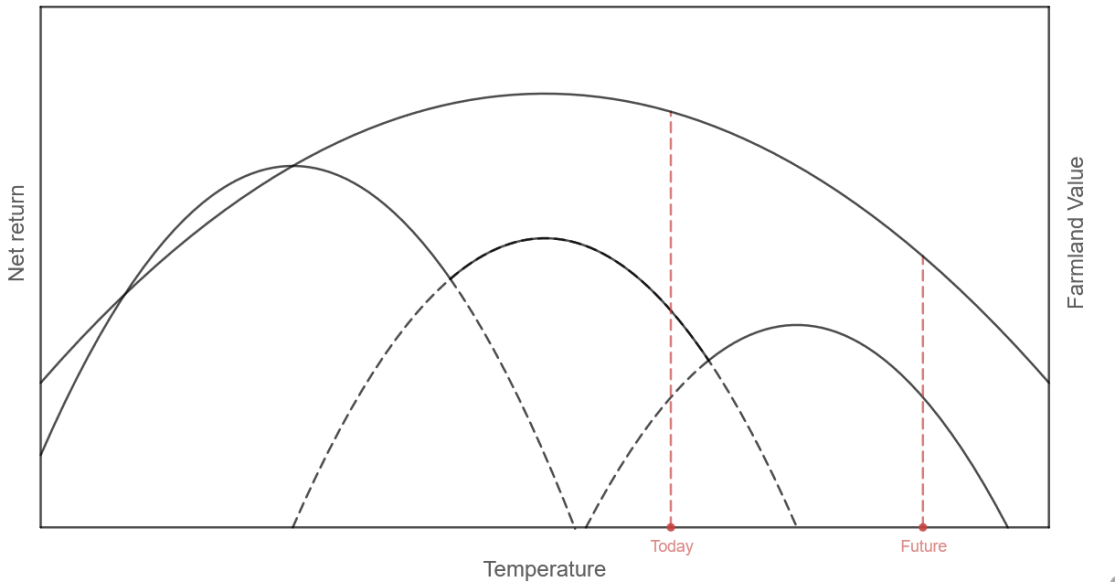

(a) Spatial homogeneous responses

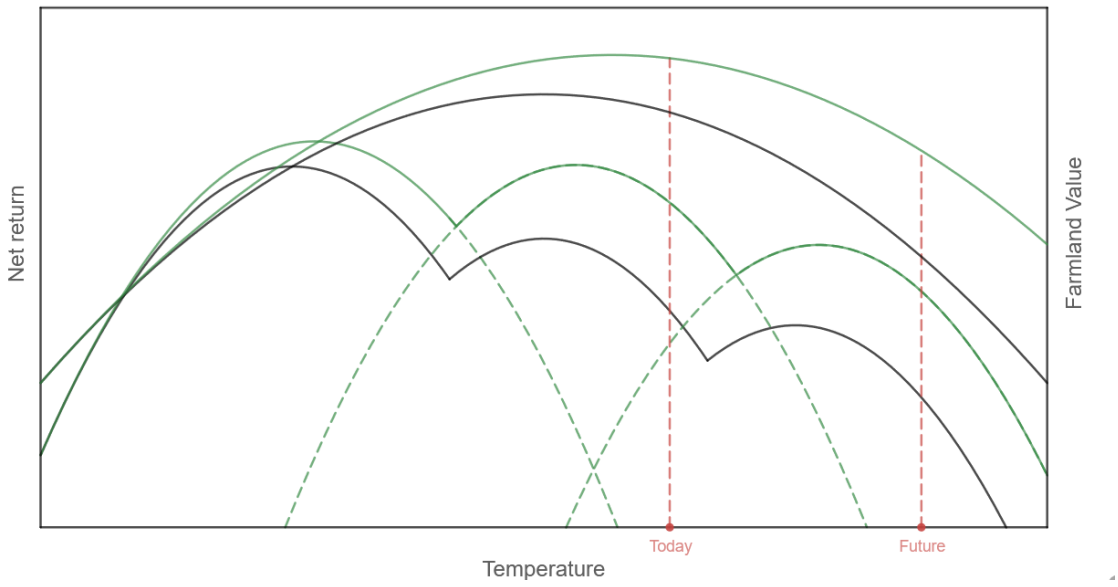

(b) Spatial heterogeneous responses

Figure 1: Hedonic approach under different spatial assumptions.

Note: For each color, the three overlapping paraboles represent three different land uses, so the upper envelop maximizes net returns with respect to the different activities and temperature levels. The outer parabole represents the land value over the different temperature and illustrates the farmers' net return expectations. Panel (a) illustrates the case for homogenous responses to climate change, while panel (b) represents the case for two different responses to climate change. The assumption of homogenous responses when the data generating process exhibits heterogenous responses as in panel (b) would lead to future predictions falling between the two outer paraboles.

$$V_i = \alpha_0 + \boldsymbol{\beta_1'} \boldsymbol{C_i} + \boldsymbol{\beta_2'} \boldsymbol{C_i^2} + \boldsymbol{\gamma'} \boldsymbol{G_i} + \boldsymbol{\theta'} \boldsymbol{S_i} + \epsilon_i \tag{3}$$

The average marginal effect of climate on farmland value, $\frac{\partial V_i}{\partial C_i} = \boldsymbol{\beta_1'} + 2\boldsymbol{\beta_2'} \boldsymbol{C_i}$, is a function of $\mathbf{C}_i$. However, in this expression, both linear terms are a-spatial. Their magnitude is assumed to be valid for any county in the sample, from Florida to Minnesota, so that the only source of spatially varying marginal effects lies in the value of the covariate $\mathbf{C}_i$. Several authors have challenged the assumption that the marginal effect of climate change is constant for all locations (Mendelsohn and Dinar, 2003; Schlenker et al., 2005; Timmins, 2006). Panel (b) of Figure 1 illustrates their rationale for the simplest case of two different responses. If the econometric model omits the different responses to climate change, future farmland predictions will fall between the green and the black outer parabolas.

The slope heterogeneity illustrated in panel (b) of Figure 1 can be treated by disaggregating the estimations to a finer spatial scale. The Ricardian literature offers different grouping strategies that consist of clustering counties that are thought to be subject to similar effects from climate change. Some of the earliest investigations in this direction find that climate change has little or no effect on irrigated farmlands, suggesting that in earlier studies the gains associated with climate change are underestimated (Mendelsohn and Dinar, 2003). Once irrigation is accounted for, Schlenker et al. (2005) find that the projected climate impact estimates for rain-fed areas converge to a national annual loss of $9.62 billion. In their panel data estimation, Deschênes and Greenstone (2007) allow the climate coefficients to fully interact with irrigation and state fixed effects. Their results indicate that climate change will benefit farmers by $3.24 billion.[4] More recently, Dall'erba and Domínguez (2016) split the U.S. Southwestern counties into two groups based on the median value of elevation. Their results show that the probability of a negative future impact of climate change is larger in highland counties which are forecasted to experience heat waves more frequently than in the lowland counties.

[4] Fisher et al. (2012) find and correct several irregularities in the paper of Deschênes and Greenstone (2007), hence concluding with a negative impact of climate change on U.S. agriculture across different model specifications.

When Cai and Dall'Erba (2021) investigate the effect of the above grouping specifications on the marginal impact of climate change on farmlands, they conclude that the predicted change in farmland values varies only slightly when either irrigation or elevation is used as the criterion for grouping spatial units. Contradictory findings about the direction and/or magnitude of the impact of climate change in U.S. agriculture arising from different grouping strategies of spatial units suggest that the clustering of spatial units in such studies has an effect on the analytical results – a problem often referred to as the modifiable areal unit problem (MAUP) (Fotheringham and Wong, 1991). This effect has been recognized in the context of studies of climate-induced agricultural productivity by (Deschênes and Greenstone, 2007, 2012).

Given the unsuitability of a priori groupings of spatial units with which to demonstrate spatially heterogeneous effects of climate change on agricultural production, we take a different approach and rely on local regressions to relax the assumption that the data generating process is constant over space without having to specify any a priori regionalization of units. Several types of statistical models exist that generate locally varying responses to the same stimuli, such as the Bayesian spatially varying coefficients model (Gelfand et al., 2003; Fotheringham et al., 2017, 2021) and the frequentist multiscale geographically weighted regression approach (Yu et al., 2020a,b), although comparative studies suggest they produce similar results (Wolf et al., 2018).

We selected the latter framework because of its ease-of-use, familiarity and scalability. Equation (4) depicts a spatially varying model where y_i is the dependent variable, and x_{ik} is the k^{th} explanatory variable. This model is known as the basic-GWR or Geographically Weighted Regression. The local coefficients are denoted as $\beta_0(u_i, v_i)$ for the intercept and $\beta_k(u_i, v_i)$ for the coefficients associated with the k^{th} explanatory variable. In turn, coefficients are a function of the i^{th} observation's latitude u_i and longitude v_i. The stochastic error is denoted by ϵ_i. To retrieve the local coefficients associated with Equation (4), GWR employs a variation of the Generalized Least Squares: $\boldsymbol{\beta} = [\boldsymbol{X'W}(u_i, v_i)\boldsymbol{X'}]^{-1}\boldsymbol{X'W}(u_i, v_i)\boldsymbol{Y}$, where the diagonal weighted matrix is denoted by $\mathbf{W}(u_i, v_i)$. Because its elements depend on the location of the i^{th} observation, each

parameter is location-specific.

$$y_i = \beta_0(u_i, v_i) + \Sigma_k \beta_k(u_i, v_i) x_{ik} + \epsilon_i \tag{4}$$

One problem with basic-GWR is that it imposes the same bandwidth (i.e. the same degree of spatial heterogeneity) on each set of local parameter estimates. To remove this problem, Fotheringham et al. (2017) derive a generalization of the basic-GWR, known as Multiscale Geographically Weighted Regression (MGWR), that permits multiple local bandwidths. This model is depicted in Equation (5) where the superscript bw indicates that each set of local parameter may have a different bandiwdth, distinguishing it from Equation (4).

$$y_i = \beta_0^{bw}(u_i, v_i) + \Sigma_k \beta_k^{bw}(u_i, v_i) x_{ik} + \epsilon_i \tag{5}$$

MGWR is estimated with a back-fitting algorithm that maximizes the expected log-likelihood of each term in an additive model: $\boldsymbol{y} = \boldsymbol{\Sigma_k f_k}$, where each $\boldsymbol{f_k} = \beta_k^{bw}(u_i, v_i) x_{ik}$ in Equation (5) and $\boldsymbol{y}$ is its dependent variable (Fotheringham et al., 2017). In each iteration, the back-fitting algorithm calculates the residual $\boldsymbol{\epsilon = y - \Sigma_k f_k}$ and regresses each term of the form $\boldsymbol{\epsilon + f_k}$ against its corresponding data vector x_{ik} using the basic-GWR estimator described above until a pre-specified convergence criterion is reached.[5] Estimating the Ricardian model of Equation (3) with the capabilities of the MGWR estimator allows the estimation of the localized marginal effects of the climate conditions on agricultural production without pre-specifying any grouping of spatial units and without imposing any restriction on optimized covariate-specific bandwidths. In this framework, the global model in equation (3) relating agricultural land value to a series of covariates is depicted in Equation (6).

$$V_i = \alpha_0^{bw}(u_i, v_i) + \boldsymbol{\beta_1^{bw}}(u_i, v_i)' \boldsymbol{C} + \boldsymbol{\beta_2^{bw}}(u_i, v_i)' \boldsymbol{C^2} + \boldsymbol{\gamma^{bw}}(u_i, v_i)' \boldsymbol{G} + \boldsymbol{\theta^{bw}}(u_i, v_i)' \boldsymbol{S} + \epsilon_i \tag{6}$$

[5] MGWR inference is discussed in the appendix.

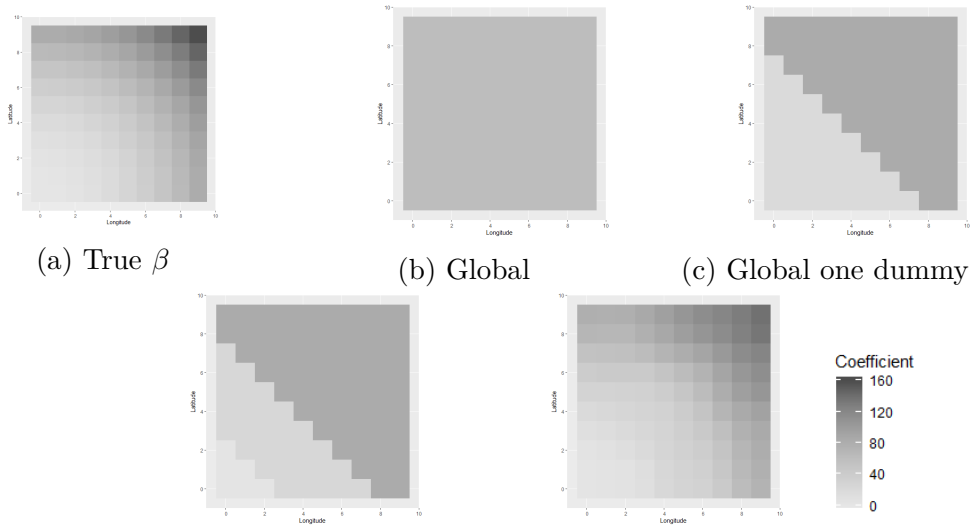

(a) True β (b) Global (c) Global one dummy

(d) Global Two dummies (e) GWR

Figure 2: Spatially varying data generating process across different estimators.
Note: True $\beta = 1 + (u_i + v_i)^2$. Panels (a) is the simulated spatial data set. Panels (b) - (d) employ different grouping techniques such that β is allowed to vary across clusters, and panel (e) is the basic-GWR estimator. As more interactions are included, global specifications improve, but they still present severe biases. The set of β values recovered with the GWR specification captures closely the true specification of β without imposing any dummy interaction.

To illustrate how local models improve upon Equation 3, panel (a) in Figure 2 shows the extreme case in which the coefficient β varies across all spatial units. Panels (b) – (d) employ different grouping techniques such that β is allowed to vary across clusters, and panel (e) is the basic-GWR estimator. As more interactions are included global specifications improve but they still present severe biases. The set of β values recovered with the GWR specification captures closely the true specification of β without imposing any dummy interaction. Panels (b) – (d) reflect the bias that ad-hoc specifications would have on local estimates while panel (e) illustrates our proposed correction. The key feature of GWR methods is therefore to allow the researcher to uncover the presence of local clusters and to include them in the estimation process without prior knowledge of the number of existing groups, group location and group membership.

3 Data

Following closely the canonical work of Mendelsohn et al. (1994), our model relates average farmland value per acre with seasonal climate data while controlling for demographic

and soil quality characteristics as shown in Equation (6). We initially considered calibrating our model with data from all 3,008 non-metropolitan contiguous U.S. counties, but we followed Schlenker et al. (2005) and Dall'erba and Domínguez (2016) by considering some counties as urban counties and hence removing 207 observations with more than 400 inhabitants per square mile from our sample. A further 34 counties were removed because of missing data for at least one of our variables. Our final sample is therefore composed of 2,687 U.S. counties.

Table 1 contains basic summary statistics related to the dependent and control variables employed in our study. Our variable of interest is the average county farmland value per acre. The U.S. Department of Agriculture prepares a census every five years in which it collects farmers' land prices. The two most recent censuses were in 2012 and 2017 and we use data from both of them in a cross-validation exercise described in the next section. The county's population density per square mile is obtained from the 2010 U.S. Census Bureau of Statistics, and the county's per-capita income is obtained from the U.S. Bureau of Economic Analysis of the same year. Controlling for socio-economic characteristics allows us to remove unwanted variation that can bias our forecast. Soil quality is a measure of a land's productivity, so we include information about salinity, flood frequency ratio, wetland, slope steepness, erosion index, sand contents, clay contents, permeability, and moisture capacity. Soil indicators are obtained from the U.S. Geological Survey.

In Table 2, we summarize our historical and forecasted climate variables. Precipitation is measured in cubic inches and temperature is measured in degree Celsius. The climate data are collected from the Parameter-elevation Regression on Independent Slopes Model (PRISM) database (PRISM Climate Group, 2021). We process PRISM data to estimate a historical average for precipitation and temperature for the U.S. counties over the 1993-2017 period. Our climate forecast scenario relies on a dynamically downscaled prediction from the North American Regional Climate Change Assessment program (NARCCAP) simulation (Mearns et al., 2013) which is derived on the basis of the A2 emission scenario from the fourth Intergovernmental Panel on Climate Change (IPCC) report. The A2

Table 1: Descriptive statistics for the value of land and control variables

Variable	Mean	s.d.	Max.	Min.
Dependent Variable				
Farmland value per acre in 2017	$3,165	$2,095	$ 28,569	$ 162
Socioeconomic Variables				
Population density per square mile	73.22	99.79	1582.74	0.13
Per capita income	$39,209	$10,531	$205,380	$18,404
Soil Quality Variables				
Salinity	0.20	0.56	7.19	0.00
Flood frequency ratio	0.08	0.12	0.73	0.00
Wetland ratio	0.55	0.38	1.00	0.00
Slope steepness	11.46	11.75	68.41	0.54
Erosion index	0.27	0.08	0.49	0.00
Sand contents	38.37	19.68	96.33	0.98
Clay content	18.54	8.15	55.12	1.12
Permeability	20.46	18.68	113.63	0.91
Moisture capacity	0.16	0.04	0.38	0.01
Observations				2,687

Note: Farmland value per acre represents the average value of all farms in a county. Farmland values and per capita income are measured in 2017 U.S. dollars.

emissions scenario assumes an increase in carbon dioxide to roughly 2.5 times the current concentration by the middle of the century (2038-2070). Both our historical climate and forecast data are estimated for the four seasons of the year to capture the variability of growing seasons in the U.S. and other potential land uses (Mendelsohn and Dinar, 2003).

Figure D.1 and Figure D.2 map the future precipitation respectively based on our climate forecast scenario by 2038-2070 for all seasons of the year. Seasonal precipitation ranges from a loss of 1.5 cubic millimeters to a gain of 1.5 cubic millimeters. Summer and Fall will become the driest seasons and Alabama, Louisiana, and Mississippi will be the most affected states. All U.S. counties are expected to experience changes in temperature of up to 5 degrees Celsius but the greatest change will be experienced in Summer in the Midwest states.

In the subsequent sections, we test the robustness of our model relative to previous specifications forecasting the impacts of climate change on agricultural land values, namely: Mendelsohn et al. (1994) (no grouping of spatial units); Schlenker et al. (2005) (two-way division of spatial units based on irrigated ratio ≥ 0.2); and Dall'erba and Domínguez (2016) (two-way division based on median elevation). For each approach we

Table 2: Historical weather and climate change scenario

Variable	Mean	s.d.	Max.	Min.
Monthly average in 1993-2017				
Temperature				
Winter (Dec. - Feb.)	2.23	6.03	19.65	-12.03
Spring (Mar. - May.)	12.88	4.90	24.74	1.21
Summer (Jun. - Aug.)	23.44	3.13	32.77	13.53
Autumn (Sep. - Nov.)	13.11	4.33	24.99	2.28
Precipitation				
Winter (Dec. - Feb.)	2.79	1.90	17.65	0.03
Spring (Mar. - May.)	3.47	1.29	10.96	0.00
Summer (Jun. - Aug.)	3.61	1.56	9.82	0.00
Autumn (Sep. - Nov.)	2.76	1.22	12.15	0.02
Difference change to mid-century (2038-2070)				
Temperature				
Winter (Dec. - Feb.)	2.24	0.57	4.25	1.29
Spring (Mar. - May.)	2.36	0.21	3.06	1.50
Summer (Jun. - Aug.)	3.41	0.40	4.32	1.84
Autumn (Sep. - Nov.)	2.89	0.26	3.27	1.80
Precipitation				
Winter (Dec. - Feb.)	0.04	0.18	0.48	-0.48
Spring (Mar. - May.)	-0.01	0.21	0.52	-0.89
Summer (Jun. - Aug.)	-0.22	0.14	0.11	-0.67
Autumn (Sep. - Nov.)	0.01	0.17	0.98	-0.49
Observations				2,689

Note: Temperature is reported in degrees Celsius. Precipitation is reported in cubic millimeters per day.

employ the same 2012 dataset to predict the 2017 farmland values. This allows us to assess the predictive power of the local regression approach described here relative to other approaches for a year for which the data are observed. We then forecast to the middle of the 22^{nd} century using all four techniques and compare the results.

4 Results

4.1 Marginal Impact of Weather on Farmland Prices

The local model in Equation (6) relating agricultural land values by county to various climate-related and socio-economic variables is calibrated using the MGWR 2.2 software available at the School of Geographical Sciences & Urban Planning at the Arizona State University (Oshan et al., 2019). In order to calibrate the model, the user must make

a choice between a fixed weighting function and a spatially adaptive one: the former is really only advisable for data on a regular lattice so here an adaptive one is used, and the optimized bandwidths are reported in terms of the number of nearest neighbors from which data are used and weighted to perform each local regression. The specific formula for the adaptive bandwidth is that of a bisquare function which is a near-normal distribution but is zero at a finite distance:

$$w_{ij} = exp\left[1 - \left(\frac{d_{ij}}{b}\right)^2\right]^2 \tag{7}$$

Figure 3 reports the MGWR parameter estimates obtained on yearly temperature and precipitation in 2017 based on Equation (6): $\sum_{k\in\Phi} \frac{\partial V_i}{\partial C_i} = \sum_{k\in\Phi} \boldsymbol{\beta_1^{bw}}(u_i, v_i)' + 2\boldsymbol{\beta_2^{bw}}(u_i, v_i)'\boldsymbol{C_i}$, where Φ corresponds to the weather variables i.e., either temperature or precipitation.[6] Panel (a) indicates the marginal effect of yearly precipitation on farmland values. Not surprisingly, most counties benefit from increases in precipitation, but as our climate forecast shows (Figure D.1), most counties will become drier. In contrast, most counties will experience losses from rising temperature as shown in panel (b), and our climate forecast indicates that all U.S. counties will become warmer (Figure D.2).

The Ricardian application of Dall'erba and Domínguez (2016) focuses on counties of the South-Western part of the US. Their work uncovers that the marginal impact of climate change is conditional on altitude. Contrary to their findings, Figure 3 shows mixed results across space for the counties east of the 100^{th} meridian. For instance, Figure 3 shows a cluster of high-value counties in West Virginia. The counties stand out for temperature only, providing evidence for the conclusions derived of Dall'erba and Domínguez (2016). The cluster does not appear for precipitation, suggesting that the impact of precipitation is not altitude-dependent. In two separate studies, Schlenker

[6]The Ricardian literature raises concerns about the non-concavity in the farmland value's responses to seasonal climate. Indeed, one should expect farmland value to increase with respect to climate at a decreasing rate as in Figure 1. This limitation prevents researchers from interpreting extremum as maximum and is the results of aggregating monthly climate into seasonal climate (Darwin, 1999).Disaggregating climate into monthly values, however, would cause serious multicollinearity issues, and dropping some arbitrary variable may cause an omitted variable bias (Mendelsohn and Massetti, 2017). Including all seasonal variables for precipitation and temperature is paramount for our analysis since we aim to capture the heterogeneity of growing seasons in the U.S.

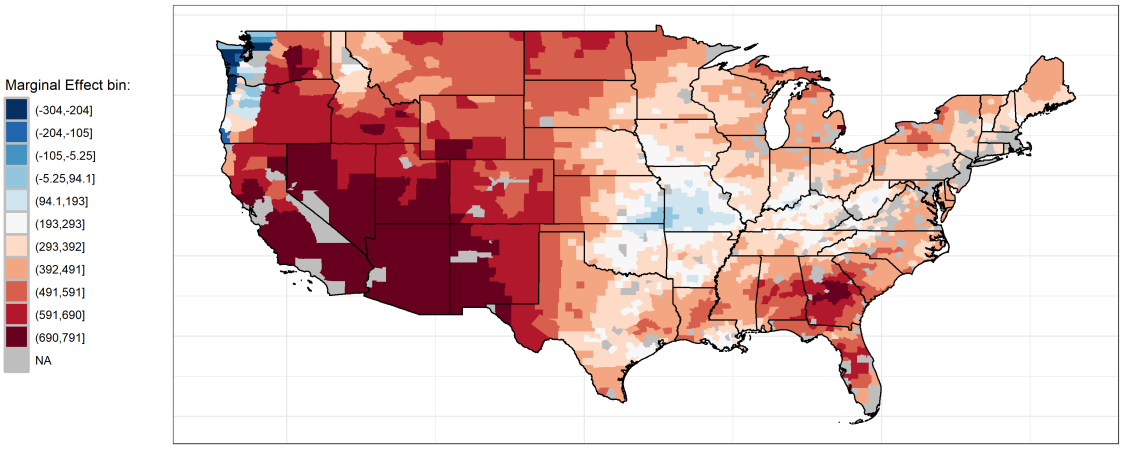

(a) Marginal Effect: Yearly Precipitation

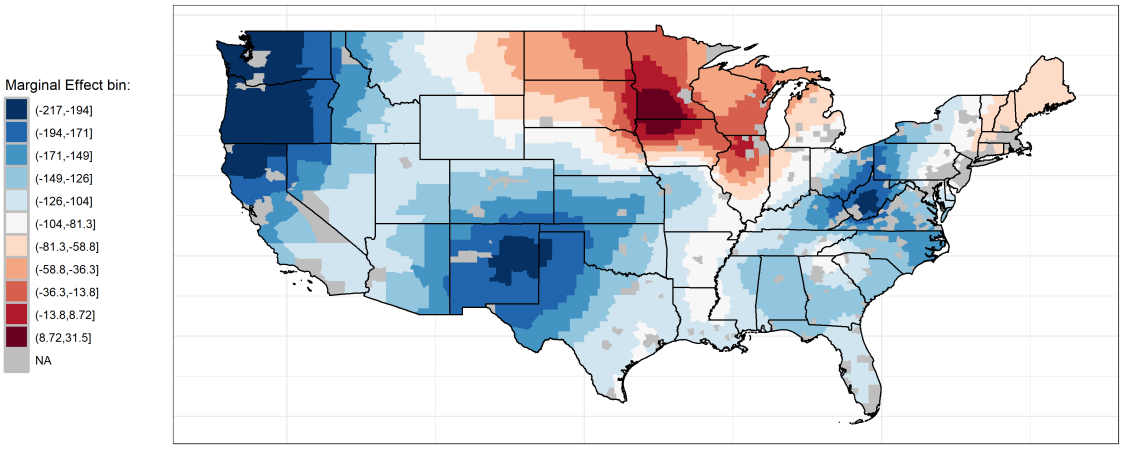

(b) Marginal Effect: Yearly Temperature

Figure 3: Marginal effect of yearly precipitation and temperature.

Note: Figure shows the yearly marginal effect of precipitation and temperature, obtained with equation 3: $\sum_{k\in\Phi}\frac{\delta V_i}{\delta C_i} = \sum_{k\in\Phi}\boldsymbol{\beta}^{bw}_{1,k}(u_i,v_i)' + 2\boldsymbol{\beta}^{bw}_{2,k}(u_i,v_i)'C_i$, where Φ indicates the variables associated with the weather variable i.e., either temperature or precipitation.

et al. (2005) and Schlenker and Roberts (2006) claim that the 100^{th} meridian should serve as an appropriate split to cluster counties. The rationale is that counties West of the 100^{th} meridian are rainfed and so more susceptible to precipitation variations. Panel (a) provides evidence to support a split by the 100^{th} meridian in terms of the impact of precipitation on farmland values. However, the marginal impact of temperature on farmland value does not display the same pattern. Indeed, panel (b) indicates the presence of substantial spatial heterogeneity in the marginal impact of temperature on both sides of the U.S. Irrigated counties west of the 100^{th} meridian show more heterogeneity. Schlenker et al. (2007) consider this phenomenon in their own Ricardian study of agriculture. Their study suggests that water availability is capitalized into land prices and concludes that farmers benefit from rain after the growing season (Fall and Winter). Our results support their conclusions. Panel (a) shows that most counties west of the 100th meridian benefit from precipitation, which replenishes aquifers. On the other hand, rain-fed counties east of the 100^{th} meridian show more heterogeneity even with some losses, suggesting that too much precipitation may lead to floods. As we previously indicated, researchers often split counties a priori by the 100^{th} meridian and include a dummy variable to generate two sets of slope coefficients. The results in Figure 3 support their rationale without needing to undertake such an arbitrary separation.

Similar to the marginal effects of climate change on farmland values, the estimated parameters associated with the demographic and soil quality variables are spatially heterogeneous. We report their distribution through histograms in Figure 4 and find large spatial variations in the estimated parameters associated with these variables, except for the demographic controls. The distribution of population density has a long tail with a bunching on the high rightmost end. This result may, in part, be driven by our exclusion of the highly populated urban areas from the sample. Per capita income shows substantial heterogeneity in its marginal impacts.

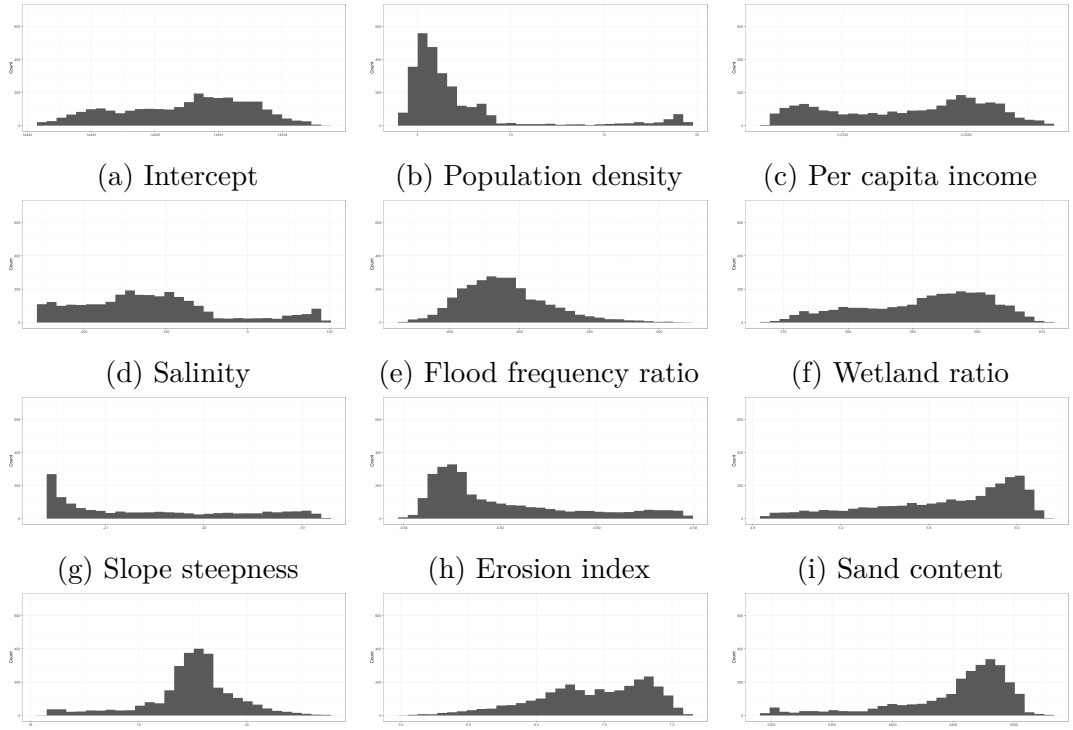

(a) Intercept (b) Population density (c) Per capita income

(d) Salinity (e) Flood frequency ratio (f) Wetland ratio

(g) Slope steepness (h) Erosion index (i) Sand content

(j) Clay content (k) Permeability (l) Moisture capacity

Figure 4: Marginal effect of demographic and soil quality variables on farmland values.
Note: Number of observations is 2,689.

4.2 Cross-Validation Results

The previous section discusses the estimation results from our MGWR application on the Ricardian model, which shows how MGWR exposes substantial heterogeneity in the marginal impact of weather on farmland values. This section is concerned with a cross-validation exercise that provides evidence about the superiority of our approach. Cai and Dall'Erba (2021) recognize the shortcomings associated with the wrongful grouping of U.S. counties in the Ricardian approach, so the authors perform cross-validation exercises across several groupings but for the same year. Our manuscript expands their approach and performs a cross-validation exercise by comparing the predictions for 2017 obtained with data from 2012 with the observed values in 2017. To this purpose, we calibrate all the models on 2012 data to predict the changes in farmland values by 2017. To our knowledge, no previous Ricardian study has used a cross-validation approach across years to demonstrate the superiority of one model over another. The results of our cross-validation exercise are depicted in Figure 5 where the observed 2012-2017 changes are

displayed on a map and in a histogram and the 2012-2017 predicted changes based on the various models are displayed below.

The table at the bottom of the figure reports certain prediction diagnostics. All the global regression models significantly underestimate the changes in farmland values. Many of the predictions from the global models are centered around zero, but with some high-valued cluster of losses, which is reflected in the average estimated county loss of -$412.08 to -$280.79 per acre. Only MGWR predicts gains between 2012-2017 with an average of $109.86, which is still lower than the observed values in 2017 at $573.92. Despite the difference, our local estimator significantly outperforms any of the global specifications as they each predict losses by 2017. The superior predictive performance of MGWR is also evidenced by its low Mean Squared Error (MSE)[7] value compared to other models.[8] Further examination of Figure 5 indicates that the results from the local model reproduces a pattern similar to the isotherms formed when temperature is mapped across latitudes in the U.S. In contrast, none of the global specifications shows this pattern, but instead they highlight ill-defined clusters of high losses.[9]

We investigate further the differences between our MGWR estimator and the global estimators in Figure 6 by dividing forecasts by climate regions (Karl and Koss, 1984).[10] This figure shows that our local estimator outperforms all global estimators across the different climate regions except for the Southern and Southeastern regions. The underperformance of global estimators is clearly observed in the Southwest and in Northwest and Central regions where all global estimators predict significantly lower values than the observed 2017 farmland values. MGWR predictions in Northwest and Central regions surpassed the observed 2017 farmland values. The absolute value of the difference between our local and the global regressions favors our MGWR application. For the Southern and Southeastern regions, the median predictions from the global estimators

[7] $MSE = \frac{1}{n}\sum_N (V_i - \hat{V}_i)^2$, where $\hat{V}_i$ is the predicted value.

[8] Our approach also ignores some outliers along the West Coast which every global estimator predict would increase slightly in 2017, suggesting that our estimator exchanges complexity in predictions for generality in the model.

[9] The MGWR predictions to the middle of the century do not follow the same temperature/latitude approach, demonstrating that our MGWR approach incorporates unspecified clusters beyond weather.

[10] Climate region divisions appear in Figure E.1.

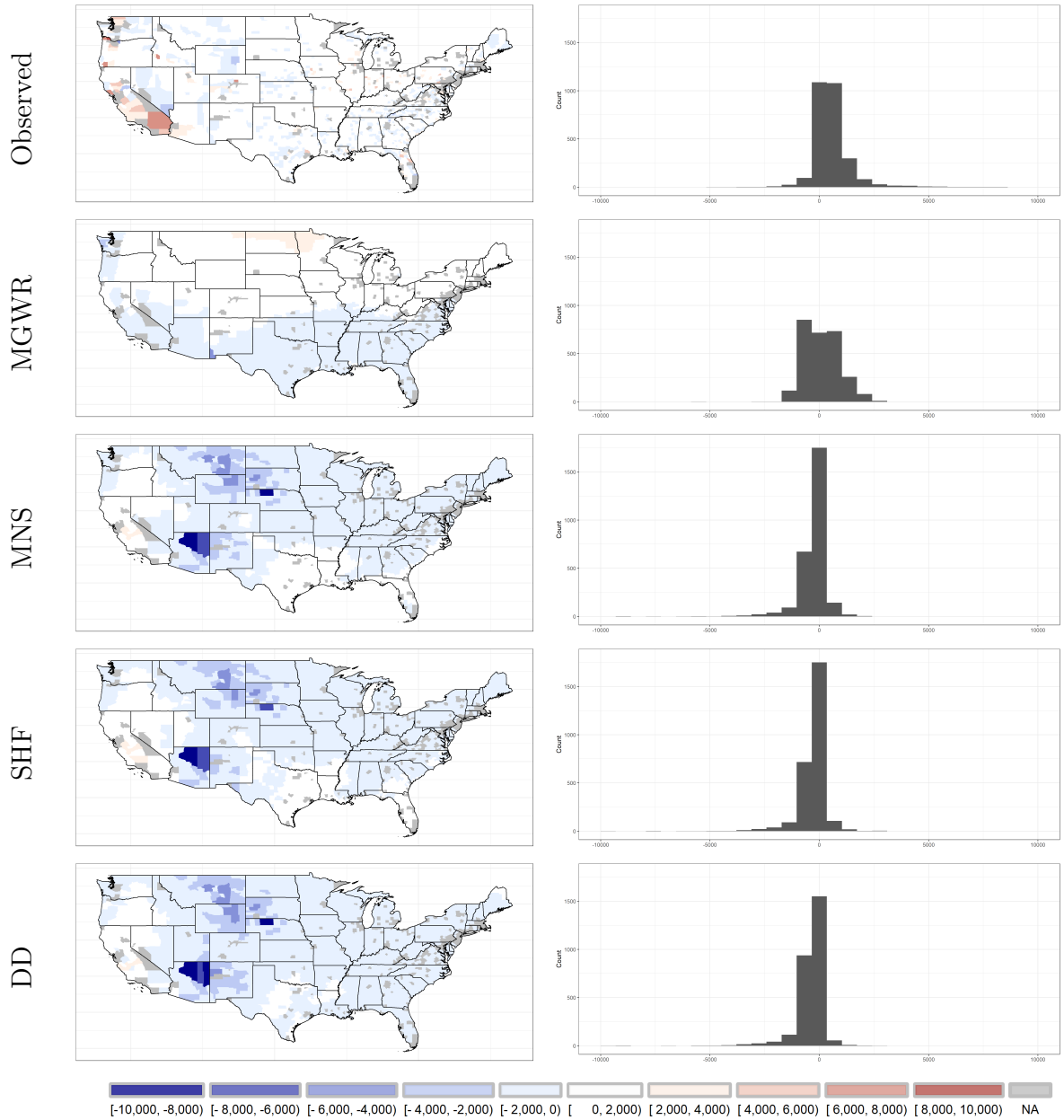

	Observed	MGWR	MNS	SHF	DD
Average gain/loss	573.92	109.86	-280.79	-285.44	-412.08
Total gains/losses	1,588,041.72	303,994	-766,938	-789,816	-1,140,231
MSE	-	2,033,204	2,241,155	2,181,644	2,490,719

Figure 5: Spatial and density distribution of observed and predicted values for 2017 across specification.

Note: MGWR is our local specification. MNS employs no grouping strategy following Mendelsohn et al. (1994). SHF splits counties by irrigation ratio (0.2) following Schlenker et al. (2005). DD splits the counties by median elevation following Dall'erba and Domínguez (2016).

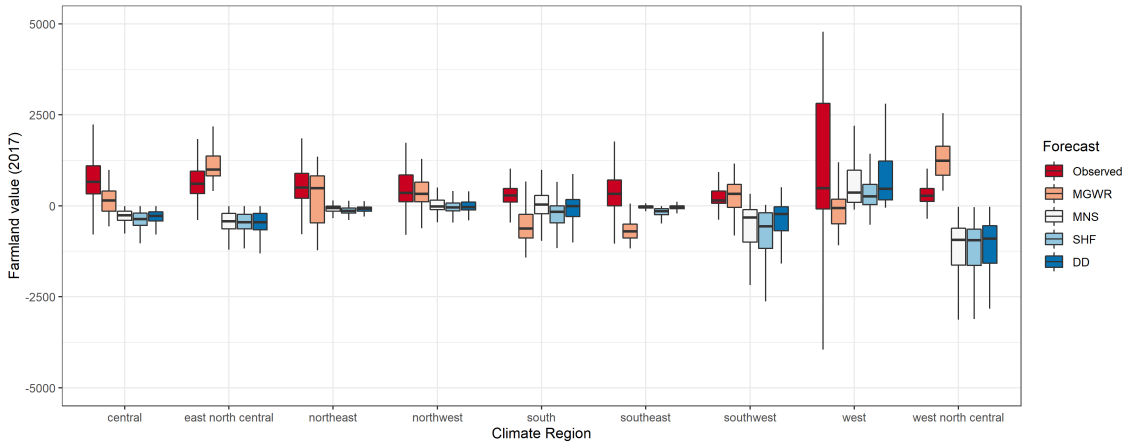

Figure 6: Observed and forecasted farmland values in 2017.

Note: Figure investigates the regional differences across estimators by dividing forecast by climate regions (Karl and Koss 1984). Outliers falling above $5,000 and below -$5,000 are trimmed for exposition.

are close to the median values of those regions with values above the average predictions, suggesting that the local estimator outperforms the global estimators.

Two additional elements can be drawn from these results. First, the local capabilities of the non-stationary Ricardian approach do not impose any kurtosis in the distribution of gains and losses. Figure 5 shows that the tails from the global predictions are thinner and longer than those from the local predictions. As a result, most global predictions fall around the mean, hence creating high peaks in their distribution. Because the non-stationary Ricardian approach does not restrict the kurtosis of our predictions, it is able to uncover important unspecified heterogeneity. The second feature we note is that local specifications ignore outliers, such as the land appreciation in the Californian counties which is likely to be a result of the California Drought of 2012. This suggests that the local model underestimates the dependent variable in the locations that are impacted by extreme weather events but still does a much better job in capturing the impacts of these events than any global model does Figure 6 shows that the regional predictions fall closer to the observed values than those predicted by global models.

5 Climate Change Impact on the U.S. Agriculture

Figure 7 describes the spatial distributions (left) and histograms (right) of our forecasted change in farmland values along with other prominent global specifications estimated using our data. MNS stands for the specification of Mendelsohn et al. (1994) that uses no grouping strategy. SHF stands for the specification of Schlenker and Roberts (2006) that splits the counties by a cutoff of 20% of the land being irrigated. DD stands for the specification of Dall'erba and Domínguez (2016) that split counties by median elevation. Our forecast predicts an average loss of -$2,239.86 per acre by 2038-2070 which is at least twice as large as the predicted average loss of MNS (-$525.26), SHF (-$575.14) and DD (-$490.60). At the national level, these figures correspond to a total loss of -$6.2 billion, which is larger than the estimates seen in the previous literature: -$1.4 billion, SHF predicts -$1.5 billion and DD predicts -$1.3 billion.

The largest losses are expected to take place among the most expensive lands located in Midwest counties; yet, the overwhelming majority of the counties will experience depreciation as climate change takes place. Our predictions suggest that some clusters of counties in Texas will benefit from climate change. In contrast to previous studies, the counties that will experience a gain from climate change are fewer in number and the gains experienced will be smaller.

Comparing the density distributions of the local predictions with those predicted from global models allows us to shine some light on the factors that determine the differences in forecasts. The large majority of changes predicted by the global models are below zero, suggesting that the substantially larger nation-wide loss we find is driven by a larger number of losers rather than by the larger magnitude of the loss. The results suggest that our MGWR application is able to capture a much greater level of variability in the responses to climate change across the U.S. We attribute these differences to omitted grouping bias in the global specification and conclude that previous global models significantly underestimate the impact of climate change on U.S. agriculture.

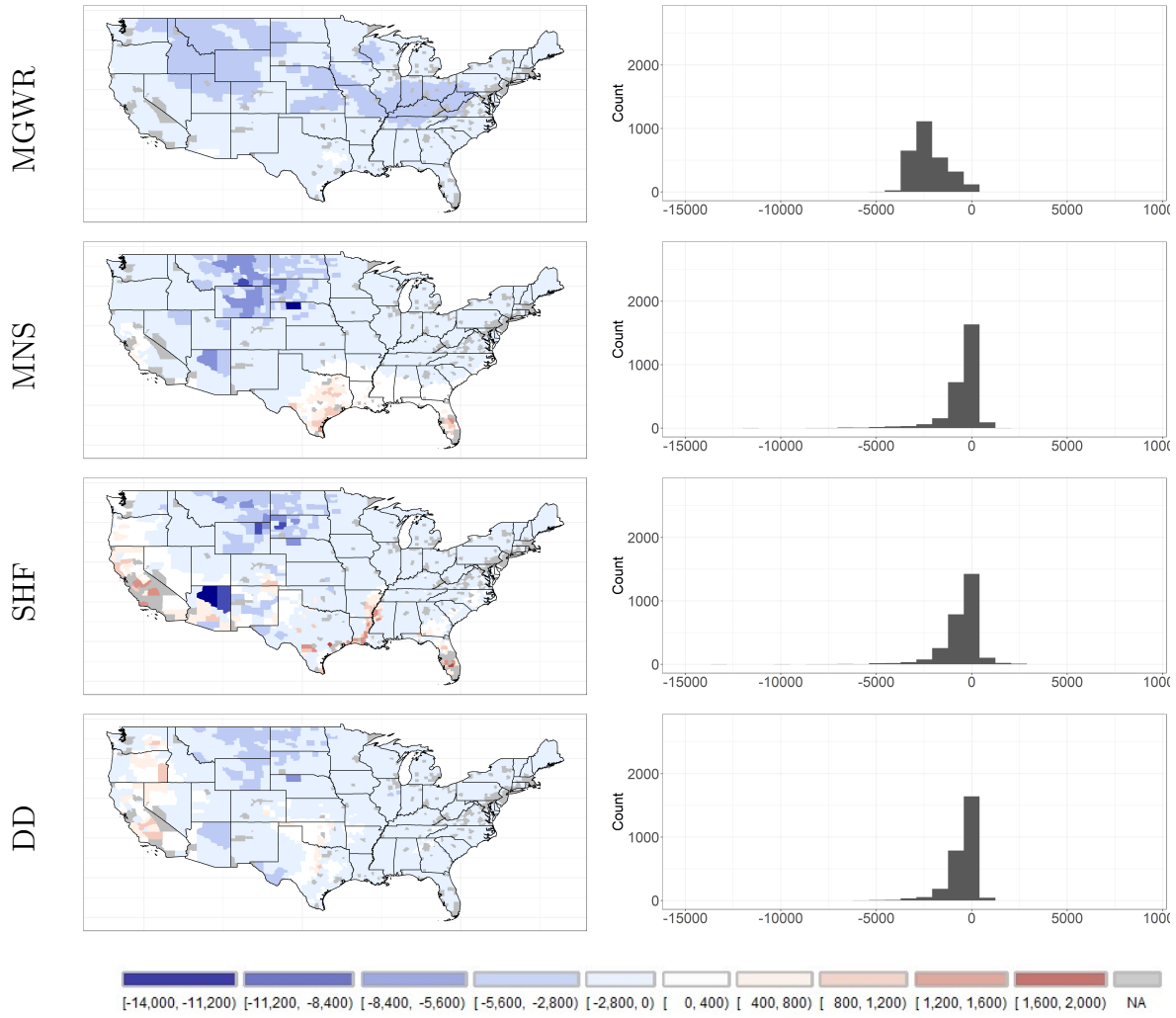

Figure 7: Spatial and density distributions of predicted land value change by the middle of the century.
Note: MGWR specification is our local specification. MNS employs no grouping strategy. SHF splits counties by irrigation ratio (0.2). DD splits counties by median elevation.

6 Conclusion

Economic estimates of the agricultural damages from climate change have largely relied on the Ricardian approach and on econometric techniques that either disregard or reduce spatial heterogeneity to a few groups. Given the size of the U.S. territory and the large variety of local climate conditions it offers, there is a suspicion that a greater degree of spatial heterogeneity is present in the impacts climate change will have on US agriculture. This paper explores this question by relying on the recently developed local statistical model MGWR. Compared to global frameworks, this modeling approach allows us to uncover spatial heterogeneity in the effects of climate change on agricultural production

without having to set a priori the number of clusters, their location and their membership; hence allowing us to generate place-specific marginal effects. Compared with global models, the MGWR forecasts exhibits a better capacity for predicting the large spatial variations in climate impact on farmland values. In addition, our results indicate that the impact of climate change on agricultural production totals a national expected average loss of -$2,239.86 per acre of farmland value across the nation, which is substantially larger than the forecasts from any previous global specification. We attribute this difference to the large heterogeneity present in the weather determinants of farmland values in combination with a wrongful a prior grouping strategy (see Figure 2). Additionally, by generating place-specific estimates, our approach offers policy makers and stakeholders a tool to address the adverse effects of climate change on a case-by-case basis. For instance, Figure 3 suggest that precipitation increases have harmful effects for the Western part of the U.S., suggesting that droughts are a concern of farmers. On the other hand, water availability in irrigated farmlands for the Eastern part of the U.S. is what concerns farmers the most. Our MGWR allows us to uncover place-specific issues related to climate distortions. Therefore, our results contrast with previous findings demonstrating that only a handful of counties, mostly located in Texas, will benefit from climate change.

Despite the novelty and strengths of our approach, we acknowledge that our approach does not include any form of interregional dependence that may place a large role in climate change mitigation. For instance, a recent contribution by Dall'Erba et al. (2021) estimates that domestic trade is able to mitigate the negative impact of climate change on crop profit by a magnitude of $14.5 billion. As such, further research most not only offer county-level predictions, but it must also account for domestic trade which has been largely ignored in the literature. Finally, this study also ignores the role of state level efforts to mitigate climate change impacts within their jurisdiction including but not limited to farm subsidies (Deschênes and Greenstone, 2007; Dall'erba and Domínguez, 2016). Due to the large array of mitigation efforts already in place, we are unable to include them in our analysis and instead we focus on the potential improvements of our MGWR application on the Ricardian approach. Future research should also pursue this

venue by including a temporal version of the MGWR, which is still not available for econometric invetigation.

References

Cai, C. and Dall'Erba, S. (2021). On the evaluation of the heterogeneous climate change impacts on U.S. agriculture: Does group membership matter? Technical report, Regional Economics Applications Laboratory.

Cai, R., Yu, D., and Oppenheimer, M. (2014). Estimating the spatially varying responses of corn yields to weather variations using geographically weighted panel regression. *Journal of Agricultural and Resource Economics*, pages 230–252.

Dall'Erba, S., Chen, Z., and Nava, N. J. (2021). US interstate trade will mitigate the negative impact of climate change on crop profit. *American Journal of Agricultural Economics*.

Dall'erba, S. and Domínguez, F. (2016). The impact of climate change on agriculture in the Southwestern United States: The Ricardian approach revisited. *Spatial Economic Analysis*, 11(1):46–66.

Darwin, R. (1999). The impact of global warming on agriculture: A Ricardian analysis: Comment. *American Economic Review*, 89(4):1049–1052.

Deschênes, O. and Greenstone, M. (2007). The economic impacts of climate change: Evidence from agricultural output and random fluctuations in weather. *American Economic Review*, 97(1):354–385.

Deschênes, O. and Greenstone, M. (2012). The economic impacts of climate change: Evidence from agricultural output and random fluctuations in weather: Reply. *American Economic Review*, 102(7):3761–73.

Fisher, A. C., Hanemann, W. M., Roberts, M. J., and Schlenker, W. (2012). The economic impacts of climate change: Evidence from agricultural output and random fluctuations in weather: Comment. *American Economic Review*, 102(7):3749–60.

Fotheringham, A. S., Li, Z., and Wolf, L. J. (2021). Scale, context, and heterogeneity:

A spatial analytical perpective on the 2016 US presidential election. *Annals of the American Association of Geographers*, pages 1–20.

Fotheringham, A. S. and Wong, D. W. (1991). The modifiable areal unit problem in multivariate statistical analysis. *Environment and Planning A*, 23(7):1025–1044.

Fotheringham, A. S., Yang, W., and Kang, W. (2017). Multiscale geographically weighted regression (mgwr). *Annals of the American Association of Geographers*, 107(6):1247–1265.

Gbetibouo, G. A. and Hassan, R. M. (2005). Measuring the economic impact of climate change on major South African field crops: A Ricardian approach. *Global and Planetary Change*, 47(2-4):143–152.

Gelfand, A. E., Kim, H.-J., Sirmans, C., and Banerjee, S. (2003). Spatial modeling with spatially varying coefficient processes. *Journal of the American Statistical Association*, 98(462):387–396.

Hsiang, S. (2016). Climate Econometrics. *Annual Review of Resource Economics*, 8:43–75.

Karl, T. and Koss, W. J. (1984). Regional and national monthly, seasonal, and annual temperature weighted by area, 1895-1983.

Liu, H., Li, X., Fischer, G., and Sun, L. (2004). Study on the impacts of climate change on China's agriculture. *Climatic Change*, 65(1):125–148.

Mearns, L., Sain, S., Leung, L., Bukovsky, M., McGinnis, S., Biner, S., Caya, D., Arritt, R., Gutowski, W., Takle, E., et al. (2013). Climate change projections of the north american regional climate change assessment program (NARCCAP). *Climatic Change*, 120(4):965–975.

Mendelsohn, R. and Dinar, A. (2003). Climate, water, and agriculture. *Land Economics*, 79(3):328–341.

Mendelsohn, R., Nordhaus, W. D., and Shaw, D. (1994). The impact of global warming on agriculture: A Ricardian analysis. *American Economic Review*, pages 753–771.

Mendelsohn, R. O. and Massetti, E. (2017). The use of cross-sectional analysis to measure climate impacts on agriculture: Theory and evidence. *Review of Environmental Economics and Policy*, 11(2):280–298.

Oshan, T. M., Li, Z., Kang, W., Wolf, L. J., and Fotheringham, A. S. (2019). mgwr: A python implementation of multiscale geographically weighted regression for investigating process spatial heterogeneity and scale. *ISPRS International Journal of Geo-Information*, 8(6):269.

Páez, A., Long, F., and Farber, S. (2008). Moving window approaches for hedonic price estimation: An empirical comparison of modelling techniques. *Urban Studies*, 45(8):1565–1581.

Plantinga, A. J., Lubowski, R. N., and Stavins, R. N. (2002). The effects of potential land development on agricultural land prices. *Journal of Urban Economics*, 52(3):561–581.

PRISM Climate Group, O. S. U. (2021). Prism Gridded Climate Data. data retrieved from PRISM website, http://prism.oregonstate.edu,.

Schlenker, W., Hanemann, W. M., and Fisher, A. C. (2005). Will U.S. agriculture really benefit from global warming? Accounting for irrigation in the hedonic approach. *American Economic Review*, 95(1):395–406.

Schlenker, W., Hanemann, W. M., and Fisher, A. C. (2007). Water availability, degree days, and the potential impact of climate change on irrigated agriculture in California. *Climatic Change*, 81(1):19–38.

Schlenker, W. and Roberts, M. J. (2006). Nonlinear effects of weather on corn yields. *Review of Agricultural Economics*, 28(3):391–398.

Shiu, Y.-S. and Chuang, Y.-C. (2019). Yield estimation of paddy rice based on satellite imagery: Comparison of global and local regression models. *Remote Sensing*, 11(2):111.

Soler, I. P. and Gemar, G. (2018). Hedonic price models with geographically weighted regression: An application to hospitality. *Journal of Destination Marketing & Management*, 9:126–137.

Timmins, C. (2006). Endogenous land use and the Ricardian valuation of climate change. *Environmental and Resource Economics*, 33(1):119–142.

Wang, J., Mendelsohn, R., Dinar, A., Huang, J., Rozelle, S., and Zhang, L. (2009). The impact of climate change on China's agriculture. *Agricultural Economics*, 40(3):323–337.

Wolf, L. J., Oshan, T. M., and Fotheringham, A. S. (2018). Single and multiscale models of process spatial heterogeneity. *Geographical Analysis*, 50(3):223–246.

Yu, H., Fotheringham, A. S., Li, Z., Oshan, T., Kang, W., and Wolf, L. J. (2020a). Inference in multiscale geographically weighted regression. *Geographical Analysis*, 52(1):87–106.

Yu, H., Fotheringham, A. S., Li, Z., Oshan, T., and Wolf, L. J. (2020b). On the measurement of bias in geographically weighted regression models. *Spatial Statistics*, 38:100453.

Zhang, H., Zhang, J., Lu, S., Cheng, S., and Zhang, J. (2011). Modeling hotel room price with geographically weighted regression. *International Journal of Hospitality Management*, 30(4):1036–1043.

Appendices

A Inference in the MGWR

Contrary to the basic-GWR, MGWR is defined as a Generalized Additive Model (GAM) whose values are estimated by a back-fitting algorithm (Fotheringham et al., 2017). In this case inference is a limitation since there is no single hat matrix mapping the estimated values $\hat{y}_i$ onto y_i that exists. Yu et al. (2020a) reframe the basic-GWR as a GAM, and demonstrate that the hat matrix for a MGWR model can be derived within the back-fitting estimation algorithm. We display their derivation, by first showing that the hat matrix for a basic-GWR can be written as an additive term. Then, we demonstrate how a hat matrix can be estimated and used for the computation of local standard errors.

The hat matrix for the basic-GWR $\boldsymbol{S}$, is defined in Equation (8) with each row given by $\boldsymbol{s_i} = \boldsymbol{X_i}(\boldsymbol{X'W}(u_i, v_i)\boldsymbol{X})^{-1}\boldsymbol{X'W}(u_i, v_i)$. Here, $\boldsymbol{X_i}$ is the i^{th} row in the matrix of all predictors $\boldsymbol{X}$.

$$\boldsymbol{S} = \begin{pmatrix} \boldsymbol{X_1}(\boldsymbol{X'W}(u_1, v_1)\boldsymbol{X})^{-1}\boldsymbol{X'W}(u_1, v_1) \\ \boldsymbol{...} \\ \boldsymbol{X_n}(\boldsymbol{X'W}(u_n, v_n)\boldsymbol{X})^{-1}\boldsymbol{X'W}(u_n, v_n) \end{pmatrix} \tag{8}$$

Let us define the additive hat matrices by $\boldsymbol{R_k}$ for the set of local parameters $\beta_{\mathbf{k}}$ associated with the kth explanatory variable, such that it has the following two properties regarding the dependent variable $\boldsymbol{y}$:

$$\hat{\boldsymbol{f}}_{\boldsymbol{k}} = \hat{\boldsymbol{R}}_{\boldsymbol{k}} y \tag{Property 1}$$

$$\hat{\boldsymbol{y}} = \boldsymbol{S}\boldsymbol{y} = \Sigma_k \boldsymbol{R_k}\boldsymbol{y} \tag{Property 2}$$

Equation (Property 1) states that $\boldsymbol{R_k}$ projects $\boldsymbol{y}$ onto each fitted additive term $\hat{\boldsymbol{f}}_{\boldsymbol{k}}$, and Equation (Property 2) implies $\Sigma_k \boldsymbol{R_k} = \boldsymbol{S}$. Next, we express each fitted additive term. Each comes from within each iteration of the back-fitting algorithm described in

the main text, as a column vector:

$$\hat{\boldsymbol{f}}_{\boldsymbol{k}} = \begin{pmatrix} x_{1k}\hat{\beta}_{1k} \\ \boldsymbol{...} \\ x_{nk}\hat{\beta}_{nk} \end{pmatrix} \tag{9}$$

Each estimated local parameter can be written as $\hat{\beta}_{ik} = \boldsymbol{e_k}\hat{\boldsymbol{\beta}}_{\boldsymbol{i}}$, where $\boldsymbol{e_k}$ is the k^{th} row of an identity matrix whose dimension is the number of regressors plus 1. Thus, we can re-write $\hat{\beta}_{ik}$ as $\hat{\beta}_{ik} = \boldsymbol{e_k}(\boldsymbol{X'W}(u_i, v_i)\boldsymbol{X})^{-1}\boldsymbol{X'W}(u_i, v_i)\boldsymbol{y}$, and Equation (9) as:

$$\hat{\boldsymbol{f}}_{\boldsymbol{k}} = \begin{pmatrix} x_{1k}\boldsymbol{e_k}(\boldsymbol{X'W}(u_i, v_i)\boldsymbol{X})^{-1}\boldsymbol{X'W}(u_i, v_i) \\ \boldsymbol{...} \\ x_{nk}\boldsymbol{e_k}(\boldsymbol{X'W}(u_i, v_i)\boldsymbol{X})^{-1}\boldsymbol{X'W}(u_i, v_i) \end{pmatrix} \boldsymbol{y} \tag{10}$$

Therefore, if the $\boldsymbol{R_k}$ is a hat matrix that projects $\boldsymbol{y}$ onto each fitted additive term $\hat{\boldsymbol{f}}_{\boldsymbol{k}}$ (Equation (Property 1)), Equation (10) allows us to write each additive hat matrix as:

$$\hat{\boldsymbol{R}}_{\boldsymbol{k}} = \begin{pmatrix} x_{1k}\boldsymbol{e_k}(\boldsymbol{X'W}(u_i, v_i)\boldsymbol{X})^{-1}\boldsymbol{X'W}(u_i, v_i) \\ \boldsymbol{...} \\ x_{nk}\boldsymbol{e_k}(\boldsymbol{X'W}(u_i, v_i)\boldsymbol{X})^{-1}\boldsymbol{X'W}(u_i, v_i) \end{pmatrix} \tag{11}$$

Now, we show how the additive hat matrix, and the MGWR hat matrix, can be estimated within the back-fitting algorithm. First, let $\boldsymbol{A_j}$ be the hat matrix of the partial model such that $\hat{\boldsymbol{f}}_{\boldsymbol{k}}^{*} = \boldsymbol{A_k}(\hat{\boldsymbol{f}}_{\boldsymbol{k}} + \hat{\boldsymbol{\epsilon}})$. Within the back-fitting algorithm, $\hat{\boldsymbol{f}}_{\boldsymbol{k}}^{*}$ is the updated fitted additive term from the previous iteration fitted additive term $\hat{\boldsymbol{f}}_{\boldsymbol{k}}$. In each iteration, the back-fitting algorithm calculates the fitted residual $\hat{\boldsymbol{\epsilon}} = \boldsymbol{y} - \boldsymbol{\Sigma_k}\hat{\boldsymbol{f}}_{\boldsymbol{k}}$; but Equation (Property 2) implies that $\boldsymbol{S} = \Sigma_k\boldsymbol{R_k}$, so we can write the following equality:

$$\hat{\boldsymbol{f}}_{\boldsymbol{k}}^{*} = \boldsymbol{A_k}(\hat{\boldsymbol{f}}_{\boldsymbol{k}} + \hat{\boldsymbol{\epsilon}}) = \boldsymbol{A_k}(\boldsymbol{R_k y} + \boldsymbol{y} - \boldsymbol{Sy}) = (\boldsymbol{A_k R_k} + \boldsymbol{A_k} - \boldsymbol{A_k S})\boldsymbol{y} \tag{12}$$

The updated additive hat matrix is $\boldsymbol{R}_{\boldsymbol{k}}^{*} = \boldsymbol{AR_k} + \boldsymbol{A_k} - \boldsymbol{A_k S}$ and the updated MGWR hat matrix is $\boldsymbol{S}^{*} = \boldsymbol{S} - \boldsymbol{R_k} + \boldsymbol{R}_{\boldsymbol{k}}^{*}$. With $\boldsymbol{R_k}$ and $\boldsymbol{S}$, local standard errors can be computed. First, let us re-write Equation (9) as $\hat{\boldsymbol{f}}_{\boldsymbol{k}} = diag(\hat{X}_k)\hat{\boldsymbol{\beta}}_{\boldsymbol{k}}$, where $diag(\hat{\boldsymbol{X}}_{\boldsymbol{k}})$

is shown in Equation (13). Then, we can re-write $\hat{\boldsymbol{\beta}}_{\boldsymbol{k}} = [diag(\boldsymbol{X_k})]^{-1}\boldsymbol{R_k y} = \boldsymbol{Cy}$, where $\boldsymbol{C} = [diag(\boldsymbol{X_k})]^{-1}\boldsymbol{R_k}$.

$$diag(\boldsymbol{X_k}) = \begin{pmatrix} x_{1k} & 0 & 0 & 0 \\ 0 & x_{2k} & 0 & 0 \\ 0 & 0 & ... & 0 \\ 0 & 0 & 0 & x_{nk} \end{pmatrix} \tag{13}$$

Finally, we can write the variances of the local parameters $\hat{\boldsymbol{\beta}}_{\boldsymbol{k}}$ as in Equation (14), where the normalized residual sum of squares from MGWR is defined by Equation (15) and the trace of $\boldsymbol{S}$ is defined by $\tau_1 = trace(\boldsymbol{S})$. Therefore, we can compute local standard errors for each parameter with: $SE(\hat{\boldsymbol{\beta}}_{\boldsymbol{k}}) = \sqrt{var(\hat{\boldsymbol{\beta}}_{\boldsymbol{k}})}$.

$$var(\hat{\boldsymbol{\beta}}_{\boldsymbol{k}}) = diag(\boldsymbol{CC'}\hat{\boldsymbol{\sigma}}^{\boldsymbol{2}}) \tag{14}$$

$$\hat{\sigma}^2 = \frac{\Sigma_N (y_i - \hat{y}_i)^2}{n - \tau_1} \tag{15}$$

The local standard errors for all local parameters estimated with the MGWR are defined by $SE(\hat{\boldsymbol{\beta}}) = [SE(\hat{\boldsymbol{\beta}}_{\mathbf{1}}, SE(\hat{\boldsymbol{\beta}}_{\mathbf{2}}), ..., SE(\hat{\boldsymbol{\beta}}_{\boldsymbol{k}},)]$, and the pseudo-t test for each local parameter is given by:

$$\frac{\hat{\beta_{ik}}}{SE(\hat{\beta_{ik}})} \sim t_{n-\tau_1} \tag{16}$$

B Farmland value forecast calculation using climate change scenario

Following Deschênes and Greenstone (2007), we define future climate as $\boldsymbol{C^1} = \boldsymbol{C^0} + \Delta$, where the superscript 1 and 0 stand for future climate and baseline climate respectively, and Δ is the change in climate from the baseline to the future. Thus, the effect of climate change on farmland values in county i yields:

$$V_i^1 - V_i^0 = \boldsymbol{\beta_1^{bw}}(u_i, v_i)'\Delta + \boldsymbol{\beta_2^{bw}}(u_i, v_i)'(2\Delta\boldsymbol{C^0} + \Delta^2) \tag{17}$$

C Data for robustness checks

Table C.1: Descriptive statistics: 2012

Variable	Mean	s.d.	Max.	Min.
Dependent Variable				
Farmland value per acre in 2012	$3,165	$2,095	$ 28,569	$ 162
Monthly average in 1993-2012				
Temperature				
Winter (Dec. - Feb.)	2.23	6.03	19.65	-12.03
Spring (Mar. - May.)	12.88	4.90	24.74	1.21
Summer (Jun. - Aug.)	23.44	3.13	32.77	13.53
Autumn (Sep. - Nov.)	13.11	4.33	24.99	2.28
Precipitation				
Winter (Dec. - Feb.)	2.79	1.90	17.65	0.03
Spring (Mar. - May.)	3.47	1.29	10.96	0.00
Summer (Jun. - Aug.)	3.61	1.56	9.82	0.00
Autumn (Sep. - Nov.)	2.76	1.22	12.15	0.02
Observations				2,689

Note: Temperature is reported in degrees Celsius. Precipitation is reported in cubic millimeters per day.

D Climate change forecast: 2038 - 2070

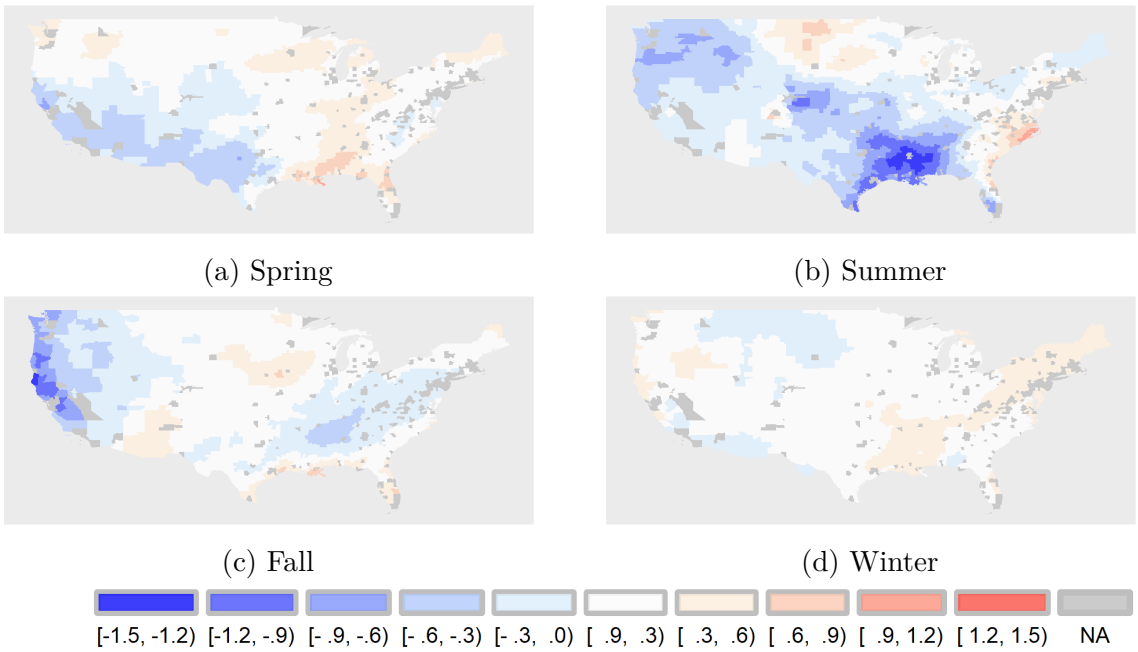

(a) Spring (b) Summer

(c) Fall (d) Winter

Figure D.1: U.S. counties climate change forecast to mid-century (2038-2070): Precipitation.

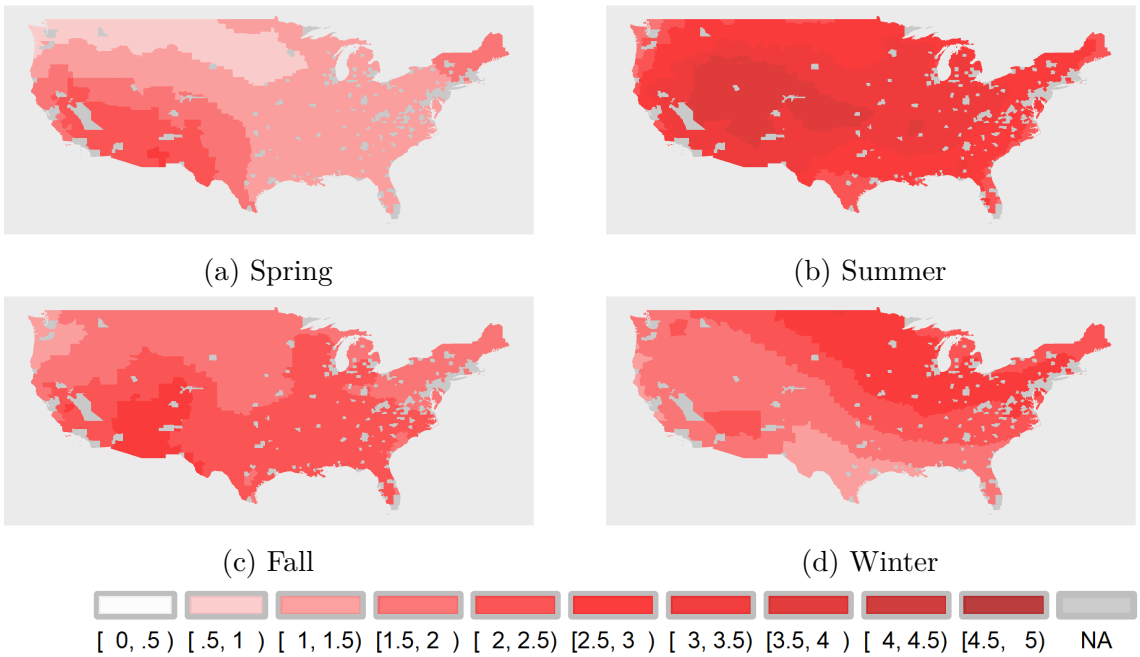

(a) Spring (b) Summer

(c) Fall (d) Winter

Figure D.2: U.S. counties climate change forecast to mid-century (2038-2070): Temperature.

E U.S. Climate Regions

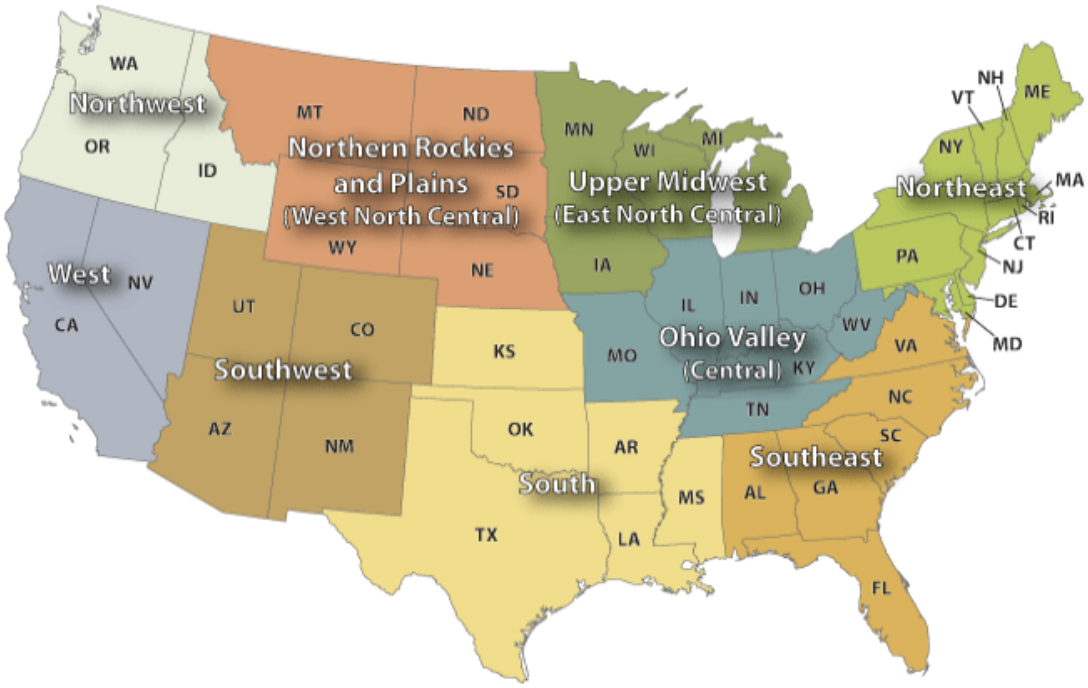

Figure E.1: U.S. Climate Regions.

Source: Karl and Koss (1984): "Regional and National Monthly, Seasonal, and Annual Temperature Weighted by Area, 1895-1983." Historical Climatology Series 4-3, National Climatic Data Center, Asheville, NC, 38 pp.